Alternative splicing of GluN1 gates glycine site–dependent nonionotropic signaling by NMDAR receptors

Hongbin Li[a] , Vishaal Rajani[a] , Lu Han[a,b], Danielle Chung[a,b], James E. Cooke[a] , Ameet S. Sengar[a] , and Michael W. Salter[a,b,1]

[a]Program in Neurosciences & Mental Health, The Hospital for Sick Children, Toronto, ON M5G 1X8, Canada; and [b]Department of Physiology, University of Toronto, Toronto, ON M5S 1A8, Canada

N-methyl-D-aspartate (NMDA) receptors (NMDARs), a principal subtype of excitatory neurotransmitter receptor, are composed as tetrameric assemblies of two glycine-binding GluN1 subunits and two glutamate-binding GluN2 subunits. NMDARs can signal nonionotropically through binding of glycine alone to its cognate site on GluN1. A consequence of this signaling by glycine is that NMDARs are primed such that subsequent gating, produced by glycine and glutamate, drives receptor internalization. The GluN1 subunit contains eight alternatively spliced isoforms produced by including or excluding the N1 and the C1, C2, or C2' polypeptide cassettes. Whether GluN1 alternative splicing affects nonionotropic signaling by NMDARs is a major outstanding question. Here, we discovered that glycine priming of recombinant NMDARs critically depends on GluN1 isoforms lacking the N1 cassette; glycine priming is blocked in splice variants containing N1. On the other hand, the C-terminal cassettes—C1, C2, or C2'—each permit glycine signaling. In wild-type mice, we found glycine-induced nonionotropic signaling at synaptic NMDARs in CA1 hippocampal pyramidal neurons. This nonionotropic signaling by glycine to synaptic NMDARs was prevented in mice we engineered, such that GluN1 obligatorily contained N1. We discovered in wild-type mice that, in contrast to pyramidal neurons, synaptic NMDARs in CA1 inhibitory interneurons were resistant to glycine priming. But we recapitulated glycine priming in inhibitory interneurons in mice engineered such that GluN1 obligatorily lacked the N1 cassette. Our findings reveal a previously unsuspected molecular function for alternative splicing of GluN1 in controlling nonionotropic signaling of NMDARs by activating the glycine site.

splicing | GluN1 | endocytosis | interneuron | nonionotropic

N-methyl-D-aspartate (NMDA) receptors (NMDARs) are heterotetrameric receptors found throughout the central nervous system (CNS) and play critical roles in neuronal development, synaptic plasticity, and disease (1, 2). NMDARs are assembled as dimers of heterodimers each composed of a glycine-binding GluN1 subunit and a glutamate-binding GluN2 subunit. Canonical signaling by NMDARs is mediated by its ionotropic function initiated through simultaneous binding of two molecules of each of the coagonists glycine (or D-serine) and glutamate to the ligand-binding domains in extracellular regions of the receptor, which produces conformational changes that open the cationic conductance pathway of the receptor complex (3, 4). However, a growing body of evidence is increasingly demonstrating nonionotropic signaling by NMDARs, signaling which is not mediated by opening of the ionic conductance pathway but which is nevertheless caused through conformational changes that are transmitted across the membrane resulting in molecular rearrangements and signaling within the cell (5–10). Nonionotropic signaling by NMDARs, often referred to as metabotropic signaling of the receptor, is increasingly implicated in development, physiology, and disease, and in novel actions of CNS drugs (11–13). A major unknown about nonionotropic signaling by NMDARs is the molecular controls on this signaling.

Here, we considered the possibility that there may be molecular control over nonionotropic signaling embedded within the structure of the NMDAR heterotetramer. We investigated this possibility by taking advantage of the naturally occurring structural diversity in the GluN1 and GluN2 subunits (3, 14). GluN1 is encoded by a single gene, *GRIN1*, with eight splice variants, whereas there are four *GRIN2* genes, encoding subunits GluN2A to D (15). Each of the GluN1 variants together with any of the GluN2 isoforms is competent to generate functional heterotetramers. Transcription and processing of *GRIN1* produces the eight messenger RNA (mRNA) variants through inclusion or exclusion of exons 5 and 21 and incorporating either exon 22 or 22' (Fig. 1*A*). The polypeptide cassettes encoded by these exons are referred to as N1, C1, C2, and C2', respectively (16, 17). The GluN1 splice isoforms are referred to as follows (15): a, N1-lacking; b, N1-containing; 1-1, C1- and, C2-containing; 1-2, C1-lacking/C2-containing; 1-3, C1- and C2'-containing; and 1-4, C1-lacking/C2'-containing (Fig. 1*A*). Many important ionotropic characteristics of NMDA receptors such as glycine and glutamate potency and voltage-dependent blockade by Mg^{2+} are unaffected by the presence of N1 insert (16–18). N-terminal splicing does affect NMDAR channel gating kinetics (19–21), as well as modulation by pH, Zn^{2+}, extracellular polyamines (22), and long-term synaptic potentiation (23). C-terminal GluN1 variants are implicated in processing NMDARs

Significance

N-methyl-D-aspartate receptors (NMDARs), which are critical in the brain, are increasingly being shown to signal without ion flux (i.e., "metabotropically"). What controls the metabotropic function of NMDARs is unknown. We discovered that a form of metabotropic signaling—glycine priming—is controlled by alternative splicing of the mRNA encoding one NMDAR subunit, GluN1. Our discovery was surprising because the spliced exon encodes a peptide cassette in the extracellular region of GluN1 far from the plasma membrane, and yet, metabotropic function requires signaling across the neuronal membrane. Moreover, we found that this metabotropic function of NMDARs is neuron cell–type specific: excitatory neurons show glycine priming, whereas inhibitory neurons do not. These findings have widespread implications for NMDARs in health and disease.

NEUROSCIENCE

Fig. 1. GluN1 splice variants regulate glycine-primed NMDAR internalization in HEK293 cells. (*A*) Schematic of the eight alternative splice variants of GluN1. (*B*) Anti-GluN1 labeling of impermeabilized HEK293 cells transfected with a GluN1 splice variant and either GluN2A or GluN2B, as indicated. Anti-GluN1 labeling was quantified using ELISA, and cell surface expression of GluN1 was calculated after receptor priming (Glycine 100 μM, 5 min) and activation (NMDA 50 μM, Gly 1 μM, 5 min) relative to control ECS. The ELISA signal from cells expressing GluN1 subunits lacking the N1 cassette decreased to a range from 42.9 ± 13.1 to $76.8 \pm 5.2\%$ of unprimed NMDARs, whereas the signal from cells expressing GluN1 subunits containing the N1 cassette remained within the range of 91.2 ± 6.8 to $129.5 \pm 24.3\%$ of unprimed NMDARs. Statistical significance is indicated with $*P < 0.05$ and $**P < 0.01$ by Student's t test. (*C*) Representative confocal microscopy images of HEK293 cells expressing recombinant NMDARs with either BBS-tagged GluN1-1a or GluN1-1b, coexpressed with either GluN2A or GluN2B. Internalized NMDAR receptors are visible in the red channel (BTX-Cypher5E) versus total NMDAR expression in the green channel (BTX-AF488). Differential interference contrast images reveal the location of cells in the corresponding field of view with conditioning glycine (Glycine 100 μM) or NMDA+glycine treatment (NMDA 50 μM, Gly 1 μM). A high resolution version of this figure can be found on Figshare (DOI: 10.6084/m9.figshare.14802654).

in the endoplasmic reticulum, Golgi, and export to the cell surface (24, 25).

A striking example of nonionotropic NMDAR signaling is that glycine binding to its cognate extracellular site on GluN1, without binding of glutamate to its cognate site, drives intracellular signaling through recruiting the AP2 endocytic adaptor complex (10, 12, 26). Activating the glycine-binding site has been shown to cause transmembrane changes resulting in conformational rearrangement of the receptor C-terminal domain (7). Given the diversity of GluN1 isoforms in the CNS and linkage of splicing to disease (23, 27), we focused on effects of alternative splicing of *GRIN1* on glycine-induced signaling by NMDARs. We examined glycine-induced signaling with all eight splice isoforms with heterologously expressed NMDARs and then with representative isoforms in mice engineered to express only GluN1a or GluN1b variants.

Results

N1 Cassette in GluN1 Prevents Glycine-Primed Internalization of Recombinant NMDARs.

To investigate whether alternative splicing of *Grin1* affects nonionotropic glycine signaling, we cotransfected HEK293 cells with one of the eight GluN1 splice variants together with either GluN2A or GluN2B. We verified that each of the constructs led to expression of protein which was trafficked to the cell surface (*SI Appendix*, Fig. S1). The enhanced AP2 association caused by glycine primes NMDARs for subsequent internalization initiated by simultaneous binding of both coagonists glycine and glutamate (10). We probed for glycine-primed internalization in two steps using a previously validated assay (26). The cells were conditioned with extracellularly applied glycine (100 μM), a concentration we previously found to prime subsequent internalization of GluN1-1a–containing NMDARs (10, 26). The cells were treated with control extracellular solution (ECS) or with ECS containing NMDA (50 μM) plus glycine (1 μM) (NMDA+glycine treatment). Cells were fixed without permeabilization, and the cell surface expression of NMDARs was quantified by enzyme-linked immunosorbent assay (ELISA). For NMDARs expressing GluN1 isoforms lacking the N1 cassette (i.e., the "a" isoforms), we found that after conditioning glycine and NMDA+glycine treatment, the surface level was significantly less than the surface level after conditioning glycine and treating with ECS (Fig. 1*B*). The glycine-primed decrease in NMDAR surface level of the "a" isoforms was observed irrespective of intracellular GluN1 C-tail variants or whether GluN1 was coexpressed with GluN2A or with GluN2B (Fig. 1*B*). By contrast, the surface levels of NMDARs expressing the "b" isoforms were not affected by conditioning glycine and NMDA+glycine treatment regardless of the GluN1 C-tail variants or coexpression with GluN2A or GluN2B. Thus, there was a striking difference between NMDAR isoforms lacking the N1 cassette, all of which showed glycine-primed internalization, as compared with isoforms containing the N1 cassette in GluN1, none of which showed glycine-primed internalization. Given this difference, we focused our subsequent investigations with recombinant NMDARs on those composed of GluN1-1a or GluN1-1b as representative of receptors, lacking or containing, respectively, the N1 cassette of the GluN1 subunit.

As an approach to test for glycine-primed internalization in addition to ELISA, we visualized changes in NMDAR surface expression by expressing GluN1 subunits in which we had inserted a bungarotoxin binding site (BBS) into the N terminus of each isoform. We have previously established for NMDARs containing GluN1-1a that BBS labeling has no effect on cell surface expression or function (26). At the beginning of each experiment, we labeled cell surface BBS-NMDARs with α-bungarotoxin (BTX) conjugated with CypHer5E, a dye which is fluorescent only in acidic pH (28), as found in the lumens of endosomes. Then, at the end of the experiment, we labeled BBS-NMDARs with BTX-conjugated Alexa Fluor 488 (BTX-AF488) to visualize NMDARs remaining on the cell surface. In cells only conditioned with glycine or only treated with NMDA+glycine, we found no CypHer5E fluorescence above background, whereas AF488 was readily detected on cells regardless of NMDAR composition (Fig. 1*C*). Thus, neither glycine alone nor NMDA+glycine alone caused endocytosis for GluN1-1a or GluN1-1b with either GluN2A or GluN2B subunits. On the other hand, bright CypHer5E fluorescence was observed in cells expressing GluN1-1a, together with GluN2A or GluN2B, following conditioning with glycine and treatment with NMDA+glycine, indicating that NMDAR endocytosis had occurred (Fig. 1*C*, *Left Lower*). However, in cells expressing GluN1-1b, conditioning with glycine and treatment with NMDA+glycine failed to drive Cypher5E fluorescence with either GluN2 subunit (Fig. 1*C*). Thus, our observations from imaging were consistent with those from ELISA, and from these convergent findings, together, we conclude that the presence of N1 cassette in GluN1 subunits prevents glycine-primed NMDAR internalization (i.e., the absence of the N1 cassette permits NMDAR internalization upon conditioning with glycine and treatment with NMDA+glycine).

N1 Cassette Prevents Glycine-Primed Depression of Recombinant NMDAR Currents.

We previously observed with recombinant NMDARs containing GluN1-1a that conditioning glycine causes a progressive, use-dependent decline of NMDA-evoked currents (10, 26). To examine the effect of the N1 cassette of GluN1 on NMDAR currents following glycine conditioning, we performed whole-cell patch-clamp recordings from HEK293 cells cotransfected with GluN1-1a or GluN1-1b together with either GluN2A or GluN2B subunits. NMDAR currents were evoked by applying NMDA (50 μM) plus glycine (1 μM) at 60-s intervals (Fig. 2). After a stable baseline current response had been established, the NMDA+glycine applications were temporarily suspended, at which time glycine in ECS or ECS was applied. The competitive glutamate-site antagonist D-APV (100 μM) was included to prevent the possibility of NMDA channel gating. We found that for the first several applications after resuming the NMDA+glycine applications, the amplitude of NMDAR currents in cells conditioned with glycine was not different from that in cells receiving ECS. Subsequently, in cells expressing NMDARs containing GluN1-1a with either GluN2A or GluN2B and conditioned with glycine+D-APV, we found that NMDAR currents progressively decreased in amplitude. The level of the currents 20 min after conditioning was significantly less than that of NMDAR currents from cells conditioned with ECS+D-APV without glycine (Fig. 2 *A* and *B*). By contrast, in cells expressing GluN1-1b together with GluN2A or with GluN2B, applying glycine+D-APV did not cause a significant decline in evoked current versus applying the ECS+D-APV control (Fig. 2 *C* and *D*). Taking these findings together, we conclude that inclusion of the N1 cassette in GluN1 prevents the glycine-primed decrease of NMDAR-mediated currents.

N1 Cassette Prevents Glycine-Primed Recruitment of AP2 to Recombinant NMDARs.

The hallmark of glycine priming of NMDARs is recruitment of the AP2 protein complex upon glycine stimulation, which readies the receptor for subsequent internalization (10). Therefore, we investigated whether including the N1 cassette of GluN1 affects glycine-stimulated recruitment of AP2. To this end, we immunoprecipitated the β-2 subunit of AP2 from HEK293 cells expressing GluN1-1a or GluN1-1b together with GluN2A or GluN2B after conditioning with glycine+D-APV or only D-APV in ECS (Fig. 2 *E–G*). With cells expressing GluN1-1a, conditioning with glycine led to a significant increase in the amount of this GluN1 subunit coimmunoprecipitating with AP2. Conditioning with glycine increased coimmunoprecipitation of GluN1-1a in cells cotransfected with GluN2A or with GluN2B. However, glycine conditioning did not change the amount of GluN1-1b–containing NMDARs coimmunoprecipitating with AP2 (Fig. 2 *E–G*).

Overall, for recombinantly expressed NMDARs, we found that including the N1 cassette in GluN1 prevents the following: 1) glycine-primed loss of NMDARs from the cell surface, 2) glycine-primed internalization of NMDARs into acidic organelles, 3) glycine-primed decline of NMDAR currents, and 4) glycine-stimulated recruitment of AP2 to the NMDAR complex. That is, the indicia of glycine priming (13) are prevented by the N1 cassette of GluN1 in heterologously expressed NMDARs activated by exogenous agonists.

Glycine Primes a Decline in Synaptic NMDAR Currents in Hippocampal CA1 Pyramidal Neurons from Rats and Mice.

To assess the effect of glycine on native NMDARs activated endogenously, we investigated NMDAR excitatory postsynaptic currents (EPSCs) in CA1 pyramidal neurons in ex vivo hippocampal slices. NMDAR EPSCs were pharmacologically isolated by blocking AMPA and GABA$_A$ receptors with bath-applied CNQX and bicuculline, respectively.
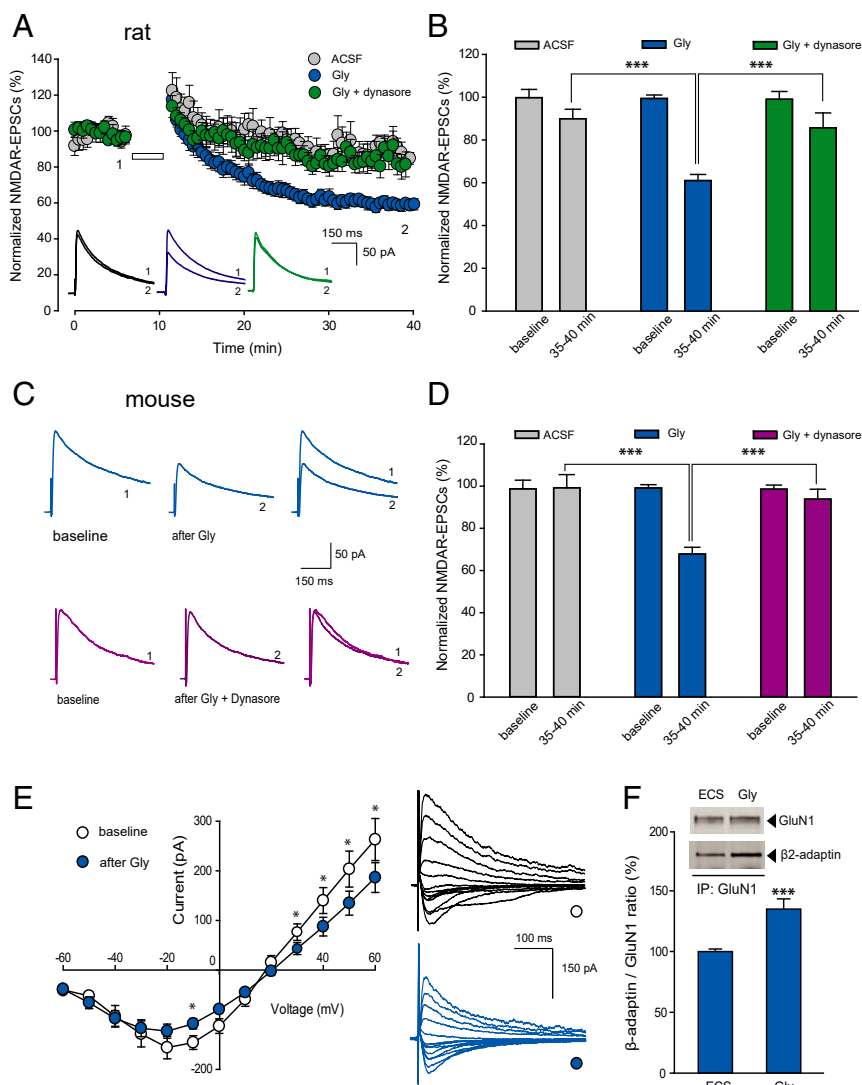
NEUROSCIENCE
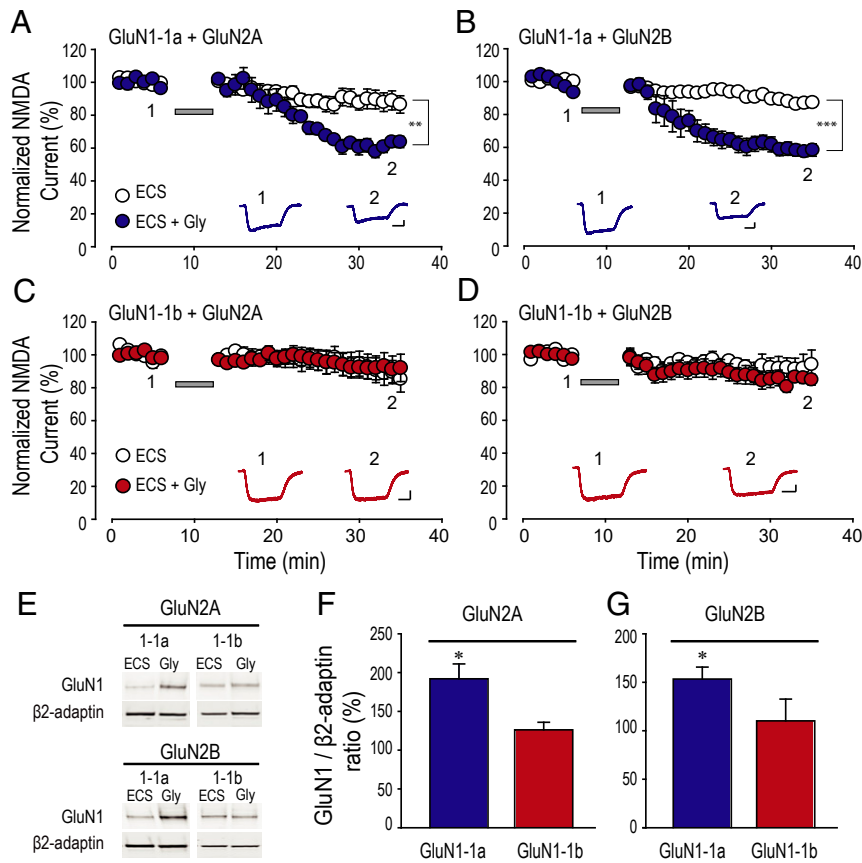
Fig. 2. N1 cassette prevents the glycine priming–induced decrease of NMDAR current in HEK293 cells. Time series of normalized NMDAR peak current evoked by 50 μM NMDA and 1 μM glycine following conditioning treatment with ECS containing 100 μM glycine and D-APV (Gly, filled circles) or ECS containing D-APV (open circles) from HEK293 cells expressing the following: (A) GluN1-1a/GluN2A receptors (58.9 ± 3.8 versus $88.4 \pm 5.8\%$, $n = 6$ and 7, respectively, $**P < 0.01$); (B) GluN1-1a/GluN2B receptors (58.1 ± 3.8 versus $87.3 \pm 2.5\%$, $n = 5$ and 7, respectively, $***P \leq 0.001$); (C) GluN1-1b/GluN2A receptors (91.3 ± 8.6, versus 88.6 ± 8.0, $n = 4$ and 5 per group); and (D) GluN1-1b/GluN2B receptors ($84.8 \pm 3.5\%$ versus 92.5 ± 8.6, $n = 5$ and 4, respectively). All values are calculated from the end of each recording. Bath application is denoted by the gray bar. At the *Bottom* of each panel are representative averaged traces from five consecutive evoked currents at the indicated times (1, 2). (Scale bar, 100 pA, 1 sec.) (E) Representative immunoblot of GluN1 and β2-adaptin after immunoprecipitation by anti–β2-adaptin of HEK293 cell lysates expressing GluN1-1a or GluN1-1b together with GluN2A (*Top*) or GluN2B (*Bottom*) after cells were conditioned with ECS+D-APV or ECS+glycine+D-APV. (F and G) Histogram of average GluN1/β2-adaptin ratio following conditioning with 100 μM glycine and D-APV in HEK293 cells expressing (F) GluN1-1a/GluN2A ($191.9 \pm 19.2\%$) versus GluN1-1b/GluN2A ($126.1 \pm 9.8\%$, $*P < 0.05$) and (G) GluN1-1a/GluN2B ($153.3 \pm 12.3\%$) versus GluN1-1b/GluN2B ($110.2 \pm 22.5\%$, $*P < 0.05$). Student's *t* test is used for all statistic comparisons.

Synaptic responses were evoked by stimulating Schaffer collateral inputs every 10 s; NMDAR EPSCs were recorded with the membrane potential held at +60 mV. After establishing a stable baseline amplitude of NMDAR EPSCs, we conditioned the slices by bath applying glycine in artificial cerebrospinal fluid (ACSF) or ACSF alone (e.g., Fig. 3A). In recordings from pyramidal neurons in slices from Sprague–Dawley rats, we found that glycine conditioning led to a gradual decrease in NMDAR EPSC amplitude to a level significantly less than that observed with conditioning with ACSF alone (Fig. 3 A and B). To test whether the decline in NMDAR EPSCs was mediated by dynamin (13), we made recordings in which the intracellular solution was supplemented with dynasore (50 μM), a small molecule inhibitor of dynamin (29). We found that, during recordings in which dynasore was included in the intracellular solution, conditioning with bath-applied glycine did not induce the decline in NMDAR EPSC amplitude observed in recordings lacking intracellular dynasore (Fig. 3 A and B). We noted that just after resuming the Schaffer collateral stimulation, the amplitude of NMDAR EPSCs from all treatment conditions had increased slightly, as compared with the baseline level. This slight and transient increase of NMDAR EPSCs might have resulted from the cease of presynaptic stimulation for the duration of glycine treatment because the magnitude of increase was indistinguishable

from all treatment conditions and the EPSCs returned to baseline within two minutes (Fig. 3A). The transient increase in EPSCs was not observed when stimulation was continued during the glycine application. Therefore, we used this approach in the remainder of our studies.

In hippocampal slices from wild-type (WT) C57BL/6 mice, we observed that conditioning with bath-applied glycine produced a significant decrease in NMDAR EPSCs in CA1 pyramidal neurons (Fig. 3 C and D). As in rat CA1 neurons, intracellular application of dynasore via the patch pipette prevented the glycine-primed decrease in NMDAR EPSCs (Fig. 3 C and D). We compared the current–voltage relationship and reversal potential of NMDAR-EPSCs at the beginning and the end of each recording and found that glycine conditioning reduced the slope conductance but did not change the reversal potential (Fig. 3E). In addition, we found that glycine treatment led to a decrease of NMDAR EPSCs in neurons recorded continuously at holding potential of −10 mV (*SI Appendix*, Fig. S2). Thus, the glycine-primed depression did not depend upon the neuron membrane potential being held at +60 mV, and this depression was not caused by a change of driving force for NMDARs. To test the possibility that conditioning with glycine might non-specifically depress excitatory synaptic transmission at Schaffer-CA1 pyramidal neuron synapses, we examined pharmacologically

Li et al.
Alternative splicing of GluN1 gates glycine site–dependent nonionotropic signaling
by NMDAR receptors

Fig. 3. Glycine-primed decline in synaptic NMDAR current is dynamin dependent in rats and mice. (*A*) Scatter plot of NMDAR EPSC peak amplitude over time from rat CA1 pyramidal neurons recorded following 5 min of bath-applied ACSF (gray), glycine (Gly 0. 2 mM, blue), or glycine (0.2 mM) with intracellularly applied dynasore (50 μM, green). Bath application is denoted by the white bar. Representative average NMDAR EPSC traces were recorded at membrane potential of +60 mV at the times indicated (1, 2). (*B*) Histogram of averaged NMDAR EPSCs measured before (baseline) and after treatment of ACSF (89.9 ± 4.4%, $n = 6$, gray), glycine (61.0 ± 2.9%, $n = 12$, blue, ***$P \leq 0.001$ versus ACSF), or dynasore (85.7 ± 6.9%, $n = 6$, green, ***$P \leq 0.001$ versus glycine, one-way ANOVA). (*C*) Representative average NMDAR EPSC traces from mouse CA1 pyramidal neurons recorded at baseline and 20 min after bath-applied treatment of glycine (Gly 1 mM, 10 min, blue) or glycine plus dynasore (50 μM in intracellular solution, purple). (*D*) Histogram of average NMDAR EPSC peak amplitudes measured before (baseline) and after treatment with ACSF (98.9 ± 4.1%, $n = 6$, gray), glycine (67.7 ± 3.6%, $n = 15$, blue, ***$P \leq 0.001$ versus ACSF), and intracellularly applied dynasore (94.0 ± 4.7%, $n = 6$, green, ***$P \leq 0.001$ versus glycine, one-way ANOVA). (*E*) Scatter plots with representative traces showing the current (I)–voltage (V) relationship and reversal potential of NMDAR EPSCs before (white) and 25 min after glycine treatment (1 mM, 10 min, blue). Statistical significance (*$P < 0.05$) was detected at holding potential of −10 mV, +30 mV, +40 mV, +50 mV, and +60 mV ($n = 12$, $P < 0.05$ between two plots, two-way ANOVA). (*F*) Histogram of averaged β2-adaptin/GluN1 ratio with glycine treatment (Gly 1mM, 10min) in hippocampal slices from wild-type mice (135.0 ± 8.10%, $n = 13$, ***$P \leq 0.001$ versus ECS, Student's *t* test). (*Top*) Representative immunoblot of GluN1 and β2-adaptin after anti-GluN1 immunoprecipation.

isolated AMPAR EPSCs (*SI Appendix*, Fig. S3). We found that conditioning with bath-applied glycine had no effect on the synaptic AMPAR responses and thus glycine did not cause depression of excitatory transmission nonspecifically. We take these findings together as evidence that glycine primes a persistent, dynamin-dependent depression of NMDAR EPSCs at Schaffer pyramidal neuron synapses in CA1 in rats and mice.

Glycine Stimulation Drives Association of AP2 with NMDARs from Wild-Type Mouse Hippocampal Slices. As glycine primes a decline in synaptic NMDAR currents in hippocampal CA1 pyramidal neurons from rats and mice, we wondered whether glycine caused recruitment

of AP2 to the NMDAR complex in the hippocampus. We used coimmunoprecipitation of AP2/NMDAR complexes from hippocampal slices from wild-type C57BL/6 mice. Slices were conditioned with either control ECS or ECS+glycine in the presence of D-APV. We observed that glycine conditioning induced a significant increase in AP2/NMDAR association in mouse slices (Fig. 3*F*), which is consistent with our previous observation that glycine conditioning enhances the association of AP2 with NMDARs in rat hippocampal slices (10). From our findings, we conclude that glycine conditioning primes depression of synaptic NMDAR currents and enhances association of AP2 with the NMDAR complex for native receptors.

Li et al.
Alternative splicing of GluN1 gates glycine site–dependent nonionotropic signaling by NMDAR receptors

PNAS | 5 of 11
https://doi.org/10.1073/pnas.2026411118

N1 Cassette of GluN1 Prevents Glycine-Primed Decline in Synaptic NMDAR Currents in Hippocampal CA1 Pyramidal Neurons. In the adult rodent hippocampus, *Grin1* mRNA is a mixture of transcripts that contain or that lack exon 5 (30, 31). Thus, native NMDARs are predicted to be a mixture in which there are receptors with GluN1 subunits containing the N1 cassette and those with GluN1 lacking this cassette. That synaptic NMDARs are normally composed of a mixture of N1-containing and N1-lacking GluN1 is consistent with findings comparing wild-type mice with genetically modified mice either constitutively lacking *Grin1* exon 5 (*Grin1*$^{\Delta 5}$ termed GluN1a mice; Fig. 4A) or obligatorily expressing *Grin1* exon 5 (*Grin1*$^{\Omega 456}$ termed GluN1b mice) (21, 23). To investigate the role of the N1 cassette of GluN1 in glycine-primed depression of synaptic NMDARs at Schaffer collateral synapses onto pyramidal neurons, we compared the effects of glycine conditioning on NMDAR EPSCs in GluN1a versus GluN1b mice. Such a comparison is experimentally appropriate because basal synaptic transmission at these synapses in GluN1a mice is not different from basal transmission in GluN1b mice (21, 23). Here, we found that glycine conditioning led to a significant decrease in NMDAR EPSCs in CA1 pyramidal neurons in hippocampal slices from GluN1a mice (Fig. 4 A and B). The proportionate depression of NMDAR EPSCs caused by conditioning glycine in GluN1a pyramidal neurons was not different from that of the glycine-primed depression in the wild type (Fig. 4B). In contrast to GluN1-1a, in CA1 pyramidal neurons in slices obtained from the GluN1b mice, conditioning with bath-applied glycine failed to produce a change in the amplitude of NMDAR EPSCs (Fig. 4 A and B).

N1 Cassette Prevents Glycine-Primed Recruitment of AP2 to Recombinant NMDARs. As forcing GluN1 subunits to contain the N1 cassette prevented glycine-primed depression of NMDAR EPSCs at Schaffer collateral synapses, we wondered whether the absence or presence of the N1 cassette of GluN1 affects glycine-stimulated recruitment of AP2 to the NMDAR complex in the hippocampus. We used coimmunoprecipitation of AP2/NMDAR complexes from hippocampal slices from GluN1a or GluN1b mice. Slices were conditioned with either control ECS or ECS+glycine. We observed that glycine conditioning induced a significant increase in AP2/NMDAR association in slices from GluN1a mice (Fig. 4C). However, conditioning with glycine did not change AP2/NMDAR association that was observed in slices from GluN1b mice (Fig. 4C).

From our findings, we conclude that glycine conditioning primes depression of synaptic NMDAR currents and enhances association of AP2 with the NMDAR complex only for native receptors in which GluN1 subunits lack the N1 cassette. That is, expression of GluN1 subunits containing the N1 cassette prevents glycine-primed enhancement of AP2 association with NMDARs and also prevents depression of NMDAR ESPCs at Schaffer collateral synapses of pyramidal cells.

Glycine-Primed NMDAR Internalization Is Absent in Hippocampal Interneurons. Schaffer collaterals make excitatory synapses onto inhibitory interneurons, as well as onto pyramidal cells in CA1. Thus, we tested whether glycine-primed depression of NMDAR EPSCs generalizes to other excitatory synapses in CA1 hippocampus. We made whole-cell patch-clamp recordings from interneurons dispersed within the stratum radiatum. We established that neurons recorded in stratum radiatum were interneurons using current clamp mode (Fig. 5 A–C). These neurons showed a distinctive firing pattern and action potential peak amplitude in response to depolarizing current injection (Fig. 5 A and B), and the amplitude of their afterhyperpolarization was much larger than that of pyramidal cells (Fig. 5C). Moreover, dye-filled cells showed morphological characteristics of stratum radiatum interneurons (Fig. 5B). To our surprise, we found that glycine conditioning had no effect on the amplitude of NMDAR EPSCs recorded from stratum radiatum interneurons in wild-type C57BL/6J mice

(Fig. 5 D and E). The lack of effect of glycine on interneurons contrasted with recordings from pyramidal neurons in these mice where we observed that conditioning with glycine produced a gradual and sustained decrease in NMDAR EPSC amplitude (Fig. 5 D and E), as expected from our findings above. Thus, glycine-primed depression of NMDAR EPSCs does not generalize to all excitatory synapses.

We considered the possibility that the lack of glycine-primed depression of NMDAR EPSCs was due to lack of GluN1a-containing NMDARs at the Schaffer collateral synapses onto inhibitory interneurons. As such, we predicted that forcing expression of only GluN1a-containing NMDARs at these synapses would recapitulate glycine-primed depression of the synaptic NMDAR currents. Consistent with this prediction, we found that glycine conditioning caused a use-dependent, progressive decline in NMDAR EPSCs recorded from stratum radiatum interneurons in hippocampal slices taken from GluN1a mice (Fig. 5 F and G). Moreover, we found that neither the rate nor the extent of the glycine-primed decrease in NMDAR EPSCs in interneurons in GluN1a mice were different from those of the decrease in NMDAR EPSCs in pyramidal cells (Fig. 5F). Importantly, forcing expression of GluN1a-containing NMDARs did not alter the fundamental characteristics of these neurons—the firing pattern or after hyperpolarization—that differentiate them from pyramidal neurons (*SI Appendix*, Fig. S4). Hence, we were clearly recording from interneurons in the slices from GluN1a mice. Thus, preventing expression of NMDARs with GluN1b (i.e., allowing only expression of GluN1a NMDARs) abrogated the lack of glycine-primed depression of NMDAR EPSCs in interneurons in CA1 hippocampus.

D-Serine Phenocopies the Effects of Glycine on Synaptic NMDARs. For synaptic NMDARs, there is evidence that endogenous ligand for GluN1 is D-serine rather than glycine (32, 33). Therefore, we investigated whether D-serine can prime synaptic NMDARs and whether this effect depends on splicing of the GluN1 N1 cassette. In our experiments on priming synaptic NMDARs by glycine, the AMPARs antagonist CNQX was used to isolate NMDAR EPSCs. To exclude the possible effect of CNQX on the glycine binding site of NMDARs (34), in the remainder of our studies we employed NBQX, an AMPAR antagonist that does not bind to the glycine site of NMDARs (35). Using NBQX did not alter the glycine-primed depression of NMDAR EPSCs in recordings from pyramidal neurons in slices from wild-type mice (Fig. 6 A and B and *SI Appendix*, Fig. S5B). For testing D-serine, we found that applying this coagonist led to a progressive decrease in NMDAR EPSC amplitude in wild-type pyramidal neurons (Fig. 6 A and B and *SI Appendix*, Fig. S5 A and B). Strikingly, the magnitude of the decrease induced by applying D-serine was not different from that caused by glycine.

To investigate the role of the N1 cassette of GluN1 in D-serine–primed depression of synaptic NMDARs at pyramidal neurons, we compared the effects of D-serine conditioning on NMDAR EPSCs in GluN1a versus GluN1b mice. We found that D-serine conditioning led to a significant decrease in NMDAR EPSCs in pyramidal neurons in hippocampal slices from GluN1a mice (Fig. 6 C and D). In contrast to GluN1a, in pyramidal neurons in slices from GluN1b mice, bath-applied D-serine failed to produce a significant change of the amplitude of NMDAR EPSCs (Fig. 6 C and D).

In contrast to pyramidal neurons, D-serine conditioning did not produce a change in the amplitude of NMDAR EPSCs in CA1 stratum radiatum interneurons in slices from wild-type mice (Fig. 6 C and D). By contrast, we found that D-serine did cause a progressive decline in NMDAR EPSCs recorded from stratum radiatum interneurons in slices taken from GluN1a mice (Fig. 6 C and D). Thus, forcing expression of only GluN1a-containing NMDARs at these synapses recapitulated D-serine–primed depression of the synaptic NMDAR currents in interneurons. Taken
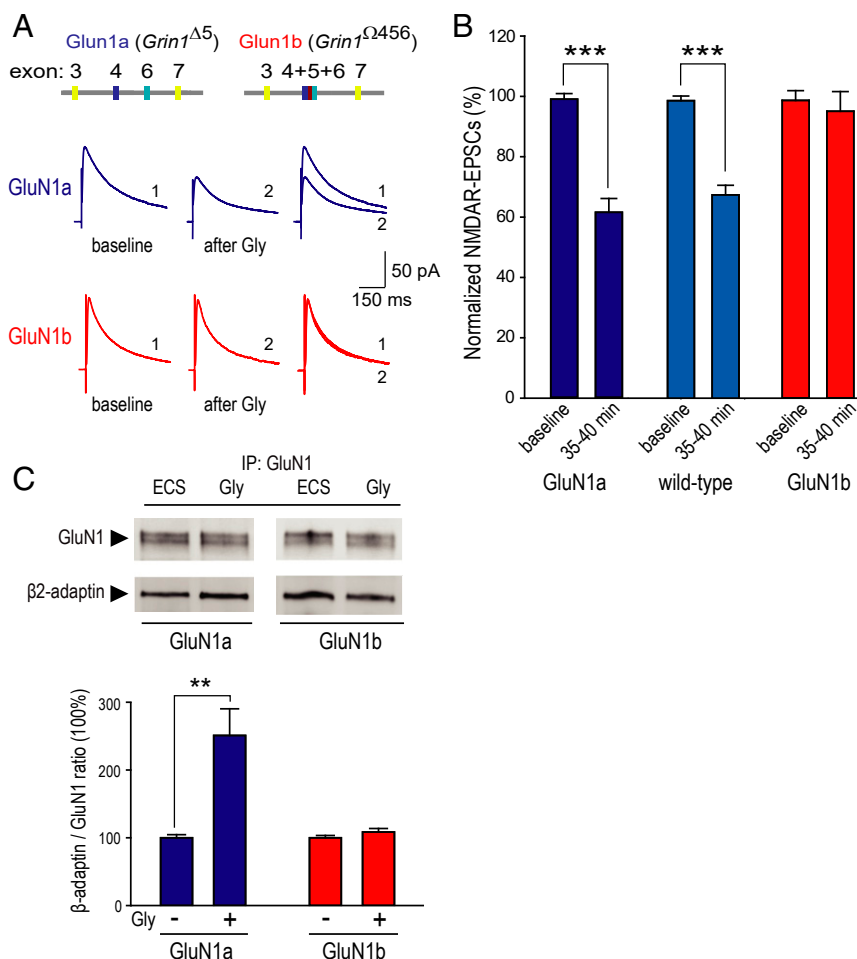
Fig. 4. Glycine-primed decline in synaptic NMDAR current is dependent on the exclusion of the N1 cassette. (*A, Top*) Schematic representation of *Grin1* loci for GluN1a and GluN1b mice depicting removal of exon 5 (*Grin1*$^{\Delta 5}$) or fusion of exons 4 to 6 (*Grin1*$^{\Omega 456}$). (*Bottom*) Representative average NMDAR EPSC traces from GluN1a (blue) and GluN1b (red) mice CA1 pyramidal neurons recorded at baseline (black) and 20 min after bath-applied treatment of glycine (Gly 1 mM, 10 min). (*B*) Histogram of averaged NMDAR EPSCs peak amplitude measured before glycine treatment as baseline and at the end of each recordings shown as the following: GluN1a (60.8 ± 4.8%, *n* = 13, ***P ≤ 0.001 versus baseline, dark blue), GluN1b (94.8 ± 4.2%, *n* = 7, *P* > 0.05 versus baseline, red), and WT (67.7 ± 3.6%, *n* = 15, blue, same data as Fig. 3*D* Gly). (*C*) Histogram of averaged β2-adaptin/GluN1 ratio with glycine treatment (Gly 1mM, 10 min) in hippocampal slices from GluN1a (250.9 ± 43.0%, *n* = 6, **P < 0.01 versus ECS, blue) and GluN1b mice (108.4 ± 5.4%, *n* = 11, *P* > 0.05 versus ECS, red). (*Top*) Representative immunoblot of GluN1 and β2-adaptin with GluN1 immunoprecipitation. Student's *t* test was used for all statistic comparisons.
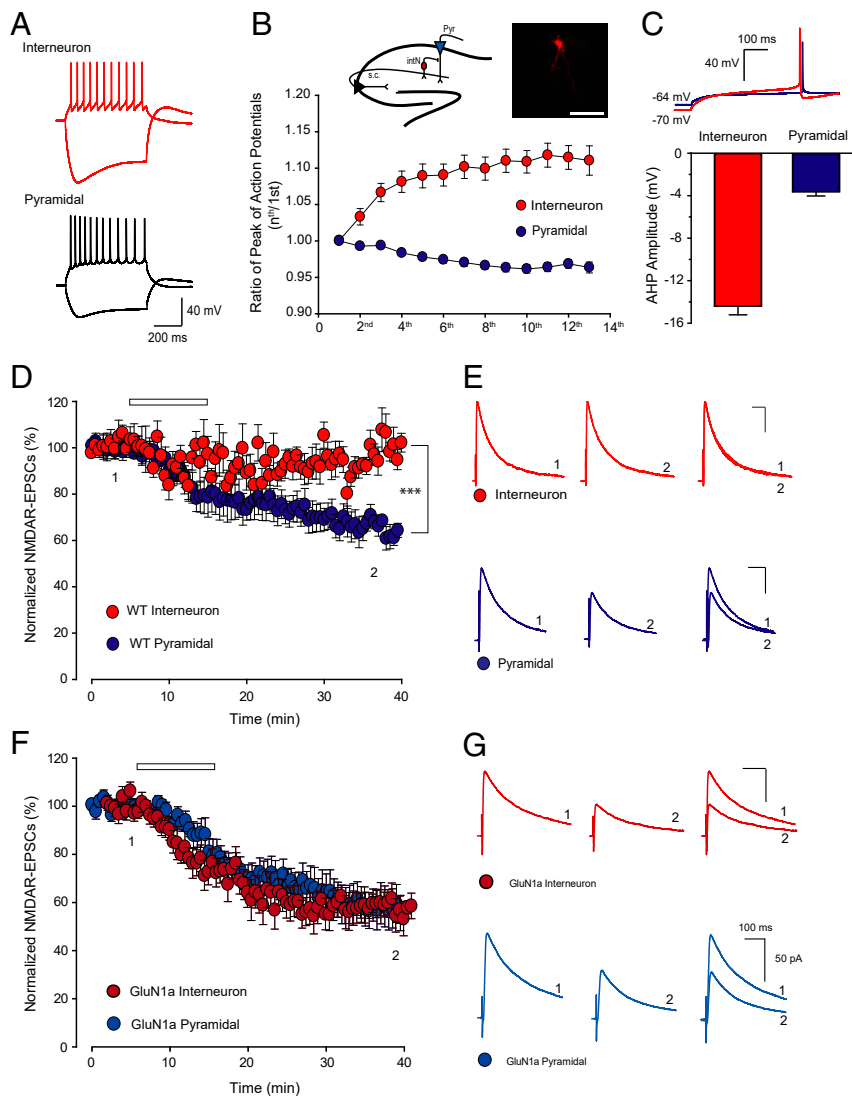
together, the findings indicate that the priming effect of D-serine in hippocampal pyramidal neurons depends on GluN1a-containing NMDARs.

The absence of glycine- or D-serine–primed depression of NMDAR EPSCs in stratum radiatum interneurons from wild-type mice may be the consequence of these neurons expressing GluN1b-containing NMDARs. As a separate approach to examine the N1 status of NMDARs at the Schaffer collateral synapses onto inhibitory interneurons, we took advantage of observations that recombinant NMDARs composed of N1 cassette–containing GluN1 exhibit faster deactivation rates than those without the N1 cassette (19, 20). In wild-type mice, we found that the decay times of the NMDAR EPSCs in pyramidal cells (230.3 ± 11.6 ms, *n* = 10) was longer than that in interneurons (162.8 ± 13.7 ms, *n* = 9, *P* < 0.05 Student's *t* test). In pyramidal cells, the decay times of NMDAR EPSCs were GluN1a > wild type > GluN1b (*SI Appendix*, Fig. S6*B*). By contrast, in interneurons, the NMDAR-EPSC decay times were GluN1a >> wild type ~ GluN1b (*SI Appendix*, Fig. S6*D*). We interpret these findings as evidence supporting the conclusion that, in interneurons in wild-type mice, synaptic NMDARs are composed predominantly, if not exclusively, of N1-containing GluN1 subunits. Thus, we conclude that the lack of glycine-primed depression of

NMDAR EPSCs in inhibitory interneurons in the wild type is due to lack of GluN1a-containing NMDARs at Schaffer collateral synapses on these interneurons.

Discussion

Here, we find that alternative splicing of *GRIN1* differentially gates glycine priming of NMDARs. Using heterologously expressed recombinant NMDARs, we observed that receptors lacking the N1 cassette in GluN1 show glycine-stimulated recruitment of AP2, glycine-primed NMDAR internalization, and glycine-primed depression of NMDAR currents. In stark contrast, we discovered that recombinant NMDARs with GluN1 containing the N1 cassette failed to show any of these three signature features of nonionotropic NMDAR signaling caused by glycine. The lack of glycine-stimulated nonionotropic signaling was observed regardless of which of the C-terminal cassettes (C1, C2, and C2') of GluN1 was present. That is to say, the permissive effect of the lack of N1 was observed, regardless of the C-terminal cassette. Moreover, the blockade glycine priming by the N1 cassette—the permissive effect of its lack—was found with recombinant NMDARs containing either GluN2A or GluN2B. Thus, the splicing of exon 5, but not splicing of other GluN1 exons, uniquely controls priming by glycine, and the effects

Li et al.
Alternative splicing of GluN1 gates glycine site–dependent nonionotropic signaling
by NMDAR receptors

PNAS | 7 of 11
https://doi.org/10.1073/pnas.2026411118

Fig. 5. Glycine-primed NMDAR internalization is inhibited in hippocampal interneurons. (*A*) Representative traces of voltage responses to hyperpolarizing current (−200 pA, 600 ms) and action potentials to depolarizing current injections recorded in CA1 pyramidal neurons (+160 pA, 600 ms) and interneurons (+60 pA, 600 ms). (*B*) Plot of average action potential peaks in a train normalized to the first action potential for both cell types. (*Inset, Left*) Diagram of a hippocampal slice showing recordings on CA1 pyramidal neuron (Pyr) and interneuron (intN) projected by Schaffer collaterals inputs. (*Inset, Right*) Two-photon imaging of an interneuron from CA1 stratum radiatum loaded with Alexa Fluor 594 via a patch pipette. (Scale bar, 100 μm.) (*C*) Histogram of after-hyperpolarization potentials (AHPs) for both cell types. (*Top*) Representative traces of single action potential and AHPs evoked by rheobase depolarizations. (*D*) Scatter plot of NMDAR EPSC peak amplitude over time from mouse CA1 pyramidal (blue) and interneurons (red) recorded with treatment of 10 min bath-applied glycine (0.2 mM, white bar). The magnitudes of NMDAR EPSCs amplitude at time point 2 were as follows: Pyr (65.5 ± 3.9%, $n = 7$) versus intN (98.9 ± 5.4%, $n = 6$, ***$P \leq 0.001$). (*E*) representative average NMDAR EPSC traces recorded at membrane potential of +60 mV at the times indicated in 1 and 2. (*F*) Scatter plot of NMDAR EPSC peak amplitude over time from GluN1a mouse CA1 pyramidal (purple) and interneurons (dark red) recorded with treatment of 10 min bath-applied glycine (0.2 mM, open bar). The magnitudes of NMDAR EPSCs amplitude at time point 2 were as follows: Pyr (57.7 ± 7.8%, $n = 6$) versus intN (57.8 ± 5.9%, $n = 6$, $P > 0.05$). (*G*) representative average NMDAR EPSC traces recorded at membrane potential of +60 mV at the times indicated in 1 and 2. Student's t test used for all statistic comparisons. A high resolution version of this figure can be found on Figshare (DOI: 10.6084/m9.figshare.14802663).

of the presence, or lack, of exon 5 occur, regardless of which GluN2 subunit the receptor is composed.

As glycine priming is initiated by binding of glycine to the receptor (13), it is conceivable that the lack of this glycine-induced nonionotropic signaling by NMDARs with the N1 cassette in GluN1 might be due simply to a lack of glycine efficacy on such receptors. We previously identified a single–amino acid substitution, A714L, in the ligand binding domain of GluN1 that likewise prevents glycine priming (26). The A714L mutation dramatically reduces the potency of glycine to induce channel gating, and this reduced binding efficacy is a simple explanation as the cause of the lack of the ability of that mutant receptor to undergo glycine

priming. However, here, neither the potency nor efficacy of glycine for its ionotropic effect (i.e., channel gating when glycine is bound to the receptor together with glutamate) are compromised in receptors containing the N1 cassette (20, 23). Thus, a simple lack of glycine binding or ability of glycine binding to stabilize an altered conformation of the receptor cannot be the mechanism for the blockade of priming by the N1 cassette. As a corollary, reduction of glycine binding is not a prerequisite to block nonionotropic signaling by GluN1.

We have proposed a schema for glycine priming of NMDARs whereby binding of glycine to its cognate site in GluN1, in the absence of binding of glutamate to GluN2, is coupled to conformational

Li et al.
Alternative splicing of GluN1 gates glycine site–dependent nonionotropic signaling
by NMDAR receptors
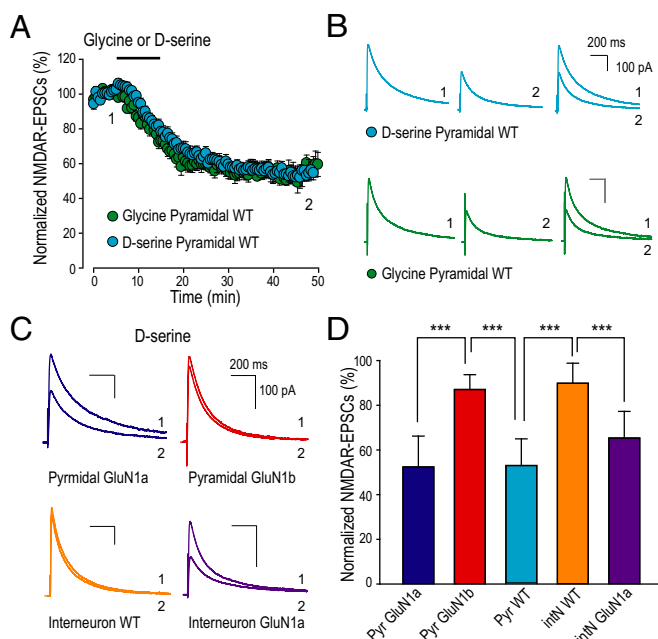
Fig. 6. D-serine primes depression of synaptic NMDARs. (*A*) Scatter plot of NMDAR EPSC peak amplitude over time from mouse CA1 pyramidal neurons recorded with 10 min treatment (black bar) of bath-applied D-serine (0.1 mM) or glycine (0.2 mM). The magnitudes of NMDAR EPSCs amplitude at time point 2 were as follows: D-serine (53.0 ± 4.0%, $n = 9$) and glycine (55.4 ± 4.0%, $n = 6$). (*B*) Representative average NMDAR EPSC traces recorded at membrane potential of +60 mV as the times indicated (1, 2) in *A* in the presence of NBQX. (*C*) Representative average NMDAR EPSC traces recorded at membrane potential of +60 mV before (1) and 30 min after D-serine treatment (2) in the presence of NBQX. Traces recorded from pyramidal neurons shown as GluN1a (blue), GluN1b (dark red), and traces from interneurons shown as wild type (orange), GluN1a (purple). (*D*) Histogram of averaged NMDAR EPSCs peak amplitude measured at 30 to 35 min after D-serine conditioning: Pyramidal neuron (Pyr) GluN1a (blue, 52.4 ± 4.9%, $n = 8$) versus GluN1b (dark red, 87.1 ± 2.7%, $n = 6$, ***$P ≤ 0.001$) and Interneuron (intN) GluN1a (purple, 65.3 ± 4.9%, $n = 6$) versus wild type (orange, 89.9 ± 3.0, $n = 9$, ***$P = 0.001$). One-way ANOVA test was used for all statistic comparisons, a statistically significant difference (***$P < 0.001$).

changes in the receptor complex initiated in the extracellular region that are transmitted across the plasma membrane where, intracellularly, these changes cause molecular rearrangement of the intracellular portions of the receptor allowing the binding of the AP2 complex (13). Such transmembrane signaling is supported by observations made by fluorescence resonance energy transfer (FRET)-based fluorescence lifetime imaging (FLIM) that D-serine rapidly induces a conformational change of the GluN1 intracellular C terminus region (7).

As a consequence of the intracellular molecular rearrangements, the AP2-bound state of the NMDAR is then able to undergo dynamin-dependent endocytosis upon the ligation of the receptor by glutamate and glycine. As we presently find that glycine does not recruit AP2 to NMDARs composed of N1-containing GluN1, we hypothesize that the N1 cassette prevents, or does not permit, the conformation rearrangements required to couple the binding glycine extracellularly to the recruitment of AP2 intracellularly. This effect of the N1 cassette could come about in a number broad conceptual ways: 1) by N1 sterically preventing the receptor from taking on the conformation (or by destabilizing this conformation) that links binding of glycine to transmembrane signaling, 2) by N1-containing receptors still signaling across the membrane but through conformational rearrangements that prevent or don't permit the intracellular binding of AP2, 3) by the presence of N1 changing extracellular or intracellular posttranslational modifications

in GluN1, or GluN2 subunits, that are necessary for transmembrane signaling or recruitment of AP2, or 4) by the presence of N1 causing changes in the composition of accessory proteins, lipids, or other molecules in the NMDAR complex–associated proteins, such that a molecule necessary for transmembrane signaling or recruitment of AP2 is missing or a molecule blocking these steps is recruited. Cryogenic electron microscopy structural data have revealed that the 21 amino acid residues of the N1 cassette are strategically positioned at the interface of the amino-terminal domain and the glycine ligand-binding domain between GluN1 and GluN2 subunits (14). This interfacial localization may support any of these four broad ways in which the N1 cassette could prevent glycine priming. Hence, our present findings open up a number of mechanistic possibilities to be addressed in the future.

Glycine-primed depression of NMDAR currents had only been previously shown for NMDAR-mediated responses evoked by exogenous agonists in acutely isolated hippocampal neurons or in spontaneous EPSCs in cells in culture (10). Here, we demonstrate that NMDAR EPSCs at Schaffer collateral synapses in CA1 pyramidal neurons in acute hippocampal slices from wild-type mice are primed by glycine or D-serine for subsequent dynamin-dependent depression when the synaptic receptors are activated. We also demonstrate that glycine treatment causes recruitment of AP2 to the NMDAR complex in mouse hippocampal slices. Thus, our present findings extend previous observations on the effects of glycine on native NMDARs and indicate that glycine priming occurs at NMDARs at synapses ex vivo.

In contrast to our findings in the wild type, in slices from GluN1b mice, NMDAR EPSCs at Schaffer collateral synapses in pyramidal neurons did not show glycine or D-serine–primed depression, nor was AP2 recruited to the NMDAR complex by glycine in GluN1b mice. On the other hand, in GluN1a mice, there was robust glycine- or D-serine–primed depression of NMDAR EPSCs at pyramidal neuron Schaffer collateral synapses and glycine-primed recruitment of AP2. Thus, as predicted from our findings with heterologously expressed recombinant NMDARs, forcing inclusion of the N1 cassette in native NMDARs prevents glycine or D-serine priming. That is, splicing out exon 5 in pyramidal neurons permits this nonionotropic signaling by activating the glycine site.

Surprisingly, given the robust and highly consistent glycine- or D-serine–primed depression of NMDAR EPSCs at Schaffer collateral synapses onto pyramidal neurons, at Schaffer collateral synapses onto interneurons in stratum radiatum in wild-type mice, glycine treatment had no effect on NMDAR ESPCs. Glycine- or D-serine–primed depression of NMDAR EPSCs in interneurons was recapitulated in slices from GluN1a mice, indicating that preventing inclusion of exon 5, and the N1 cassette, is sufficient to allow nonionotropic signaling by glycine site activation in these neurons. The lack of glycine- or D-serine–primed depression of NMDAR EPSCs and the faster decay time of NMDAR EPSCs in interneurons in the wild type and the rescue of glycine or D-serine priming in GluN1a mice, together, suggest that synaptic NMDARs in interneurons are normally composed of GluN1 subunits containing the N1 cassette; that is exon 5 is normally included in GluN1 mRNA in these neurons. This interpretation is supported by recent evidence from fluorescence-activated cell sorting (FACS)-sorted cortical neurons in which interneurons have much lower levels of GluN1 transcripts lacking exon 5 than do excitatory neurons (30). Among the major subtypes of interneurons (parvalbumin, PV; somatostatin, SST; and vasoactive intestinal polypeptide, VIP) the lowest level transcripts lacking exon 5, on average about 10%, are expressed in the PV interneurons. PV interneurons are prominent in stratum radiatum, and the very low level of exon 5-lacking transcripts in these cells is consistent with our findings of no detectable glycine-primed depression of synaptic NMDAR currents in the interneurons we recorded.

Li et al.
Alternative splicing of GluN1 gates glycine site–dependent nonionotropic signaling by NMDAR receptors

PNAS | 9 of 11
https://doi.org/10.1073/pnas.2026411118

In pyramidal cells, the level of depression of NMDAR EPSCs primed by glycine, ~40% depression, was similar to the level with recombinant receptors expressing GluN1-1a (compare Fig. 2 *A* and *B* with Fig. 3 *A* and *B*). In GluN1a mice, the degree of glycine-primed depression of NMDAR EPSCs in pyramidal neurons was not greater than that in the wild type (compare Fig. 3 *A* and *B* with Fig. 4 *A* and *B*). Thus, in pyramidal neurons in wild-type mice, the nonionotropic glycine signaling effect of GluN1 subunits lacking the N1 cassette appears to be maximal and dominates over any effect of subunits containing N1 that may be present at synapses (23). This interpretation is supported by the finding that in excitatory cortical neurons greater than 90% of GluN1, mRNA transcripts have been found to lack exon 5 (30). The differential level of exon 5 inclusion in excitatory versus inhibitory neurons—with nearly all transcripts in the former lacking exon 5 and the majority in the latter containing exon 5—provides an explanation for the dramatic increase in glycine-stimulated recruitment of AP2 to the NMDAR complex in hippocampal extracts from GluN1a versus wild-type mice (compare Fig. 3*G* and Fig. 4*D*). That is, forcing the exclusion of exon 5, and thereby the N1 cassette, in interneurons of GluN1a mice allows glycine-primed recruitment of AP2 to NMDARs in these neurons, which was absent in the wild type. Whereas in pyramidal neurons such recruitment is near maximum even in wild-type mice and neither AP2 recruitment nor glycine-primed depression of NMDAR EPSCs can be increased in these neurons in GluN1a mice.

That glycine- or D-serine–stimulated depression of NMDAR EPSCs can be prevented in pyramidal neurons in GluN1b mice and imposed on interneurons in GluN1a mice demonstrates cell-type–specific functional consequences attributable to the differences in splicing of exon 5. This differential alternative splicing in pyramidal neurons versus inhibitory interneurons may be mediated through differential action of splicing factor(s) in these two cell types. An example of one such splicing factor is the RNA-binding protein NOVA2, which has been found to control unique RNA splicing programs in inhibitory and excitatory neurons (36). The identity, or identities, of the splicing factor(s) responsible for the differential splicing of GluN1 exon 5 remains to be determined.

Differential splicing of *Grin1* exon 5 has been found to control the level of hippocampal long-term potentiation (LTP) at Schaffer collateral synapses on pyramidal neurons (23). The reduced LTP observed in GluN1b mice could not be explained by a number of factors, including basal transmission, synaptic NMDAR or AMPAR currents, NMDAR to AMPAR ratio, magnesium block potency, nor allosteric potentiation by magnesium or spermine (23). As a result, it is conceivable that nonionotropic signaling by glycine through GluN1 may be responsible for these differences and that the lack of the N1 cassette may permit transmembrane signal transduction that is necessary for LTP in hippocampal pyramidal neurons.

A consequence of the cell-type–specific differential splicing of exon 5 may be that under circumstances where glycine or D-serine are increased (37), NMDARs are unable to be down-regulated in neurons in which exon 5 and the N1 cassette are present. One such example is pathophysiological ischemia, where it is known that a subpopulation of interneurons is preferentially sensitive to death (38–40). It is conceivable that inclusion of exon 5 in these neurons makes them unable to remove cell-surface NMDARs, thereby causing their preferential sensitivity.

Additional examples of nonionotropic signaling of NMDARs stimulated by glycine or D-serine are increasingly reported (7, 32, 41). Our findings altogether uncover a previously unanticipated molecular function for the N1 cassette, encoded by exon 5, in controlling nonionotropic glycine site signaling through the GluN1 subunit of NMDARs. We suggest that differential alternative splicing of exon 5 may play important, cell-specific signaling roles as demonstrated by the distinct phenotypes between CA1 pyramidal neurons and interneurons within the hippocampus. Our findings raise the possibility that the difference in exon 5 splicing in excitatory versus inhibitory neurons generalizes throughout the CNS and may thereby have widespread consequences for NMDAR-dependent integration and circuit function.

Materials and Methods

Detailed experimental procedures on cell culture and transfection, ELISA, confocal microscopy, immunoprecipitation and immunoblot for β2-adaptin with NMDARs, whole-cell recording in recombinant NMDARs, hippocampal slice electrophysiology, and two-photon imaging are provided in *SI Appendix*.

Quantification and Statistical Analysis. All experiments were performed with at least three individual mice or cell culture wells. Number of samples used in each experiment are reported in the respective figure legends. Sigmaplot or R was used for plots and statistical analysis. All data were tested for normality before applying appropriate parametric or nonparametric test. Specific statistic tests for each experiment are reported in their respective figure legends. An alpha of 0.05 was used throughout this study. Asterisks symbolize P values as follows $*P < 0.05$, $**P \leq 0.01$, and $***P \leq 0.001$.

1. T. V. Bliss, G. L. Collingridge, A synaptic model of memory: Long-term potentiation in the hippocampus. *Nature* **361**, 31–39 (1993).
2. C. G. Lau, R. S. Zukin, NMDA receptor trafficking in synaptic plasticity and neuro-psychiatric disorders. *Nat. Rev. Neurosci.* **8**, 413–426 (2007).
3. K. B. Hansen *et al.*, Structure, function, and allosteric modulation of NMDA receptors. *J. Gen. Physiol.* **150**, 1081–1105 (2018).
4. S. F. Traynelis *et al.*, Glutamate receptor ion channels: Structure, regulation, and function. *Pharmacol. Rev.* **62**, 405–496 (2010).
5. J. Aow, K. Dore, R. Malinow, Conformational signaling required for synaptic plasticity by the NMDA receptor complex. *Proc. Natl. Acad. Sci. U.S.A.* **112**, 14711–14716 (2015).
6. K. Dore, J. Aow, R. Malinow, Agonist binding to the NMDA receptor drives movement of its cytoplasmic domain without ion flow. *Proc. Natl. Acad. Sci. U.S.A.* **112**, 14705–14710 (2015).
7. J. S. Ferreira *et al.*, Co-agonists differentially tune GluN2B-NMDA receptor trafficking at hippocampal synapses. *eLife* **6**, e25492 (2017).
8. S. Nabavi *et al.*, Metabotropic NMDA receptor function is required for NMDA receptor-dependent long-term depression. *Proc. Natl. Acad. Sci. U.S.A.* **110**, 4027–4032 (2013).
9. N. L. Weilinger *et al.*, Metabotropic NMDA receptor signaling couples Src family kinases to pannexin-1 during excitotoxicity. *Nat. Neurosci.* **19**, 432–442 (2016).
10. Y. Nong *et al.*, Glycine binding primes NMDA receptor internalization. *Nature* **422**, 302–307 (2003).
11. K. Dore, J. Aow, R. Malinow, The emergence of NMDA receptor metabotropic function: Insights from imaging. *Front. Synaptic Neurosci.* **8**, 20 (2016).
12. V. Rajani, A. S. Sengar, M. W. Salter, Tripartite signalling by NMDA receptors. *Mol. Brain* **13**, 23 (2020).
13. Y. Nong, Y. Q. Huang, M. W. Salter, NMDA receptors are movin' in. *Curr. Opin. Neurobiol.* **14**, 353–361 (2004).
14. M. C. Regan *et al.*, Structural mechanism of functional modulation by gene splicing in NMDA receptors. *Neuron* **98**, 521–529.e3 (2018).
15. P. Paoletti, C. Bellone, Q. Zhou, NMDA receptor subunit diversity: Impact on receptor properties, synaptic plasticity and disease. *Nat. Rev. Neurosci.* **14**, 383–400 (2013).
16. R. S. Zukin, M. V. Bennett, Alternatively spliced isoforms of the NMDARI receptor subunit. *Trends Neurosci.* **18**, 306–313 (1995).
17. N. Nakanishi, R. Axel, N. A. Shneider, Alternative splicing generates functionally distinct N-methyl-D-aspartate receptors. *Proc. Natl. Acad. Sci. U.S.A.* **89**, 8552–8556 (1992).
18. G. M. Durand *et al.*, Cloning of an apparent splice variant of the rat N-methyl-D-aspartate receptor NMDAR1 with altered sensitivity to polyamines and activators of protein kinase C. *Proc. Natl. Acad. Sci. U.S.A.* **89**, 9359–9363 (1992).
19. G. Rumbaugh, K. Prybylowski, J. F. Wang, S. Vicini, Exon 5 and spermine regulate deactivation of NMDA receptor subtypes. *J. Neurophysiol.* **83**, 1300–1306 (2000).
20. K. M. Vance, K. B. Hansen, S. F. Traynelis, GluN1 splice variant control of GluN1/GluN2D NMDA receptors. *J. Physiol.* **590**, 3857–3875 (2012).

21. H. Liu *et al*., N-terminal alternative splicing of GluN1 regulates the maturation of excitatory synapses and seizure susceptibility. *Proc. Natl. Acad. Sci. U.S.A.* **116**, 21207–21212 (2019).

22. S. F. Traynelis, M. Hartley, S. F. Heinemann, Control of proton sensitivity of the NMDA receptor by RNA splicing and polyamines. *Science* **268**, 873–876 (1995).

23. A. S. Sengar *et al*., Control of long-term synaptic potentiation and learning by alternative splicing of the NMDA receptor subunit GluN1. *Cell Rep.* **29**, 4285–4294.e5 (2019).

24. Y. Mu, T. Otsuka, A. C. Horton, D. B. Scott, M. D. Ehlers, Activity-dependent mRNA splicing controls ER export and synaptic delivery of NMDA receptors. *Neuron* **40**, 581–594 (2003).

25. S. Okabe, A. Miwa, H. Okado, Alternative splicing of the C-terminal domain regulates cell surface expression of the NMDA receptor NR1 subunit. *J. Neurosci.* **19**, 7781–7792 (1999).

26. L. Han, V. A. Campanucci, J. Cooke, M. W. Salter, Identification of a single amino acid in GluN1 that is critical for glycine-primed internalization of NMDA receptors. *Mol. Brain* **6**, 36 (2013).

27. N. N. Parikshak *et al*., Genome-wide changes in lncRNA, splicing, and regional gene expression patterns in autism. *Nature* **540**, 423–427 (2016).

28. E. J. Adie *et al*., A pH-sensitive fluor, CypHer 5, used to monitor agonist-induced G protein-coupled receptor internalization in live cells. *Biotechniques* **33**, 1152–1154, 1156–1157 (2002).

29. E. Macia *et al*., Dynasore, a cell-permeable inhibitor of dynamin. *Dev. Cell* **10**, 839–850 (2006).

30. M. A. Huntley *et al*., Genome-wide analysis of differential gene expression and splicing in excitatory neurons and interneuron subtypes. *J. Neurosci.* **40**, 958–973 (2020).

31. H. Raeder *et al*., Expression of N-methyl-d-aspartate (NMDA) receptor subunits and splice variants in an animal model of long-term voluntary alcohol self-administration. *Drug Alcohol Depend.* **96**, 16–21 (2008).

32. T. Papouin *et al*., Synaptic and extrasynaptic NMDA receptors are gated by different endogenous coagonists. *Cell* **150**, 633–646 (2012).

33. H. Wolosker, NMDA receptor regulation by D-serine: New findings and perspectives. *Mol. Neurobiol.* **36**, 152–164 (2007).

34. R. A. Lester, M. L. Quarum, J. D. Parker, E. Weber, C. E. Jahr, Interaction of 6-cyano-7-nitroquinoxaline-2,3-dione with the N-methyl-D-aspartate receptor-associated glycine binding site. *Mol. Pharmacol.* **35**, 565–570 (1989).

35. W. Yu, R. F. Miller, NBQX, an improved non-NMDA antagonist studied in retinal ganglion cells. *Brain Res.* **692**, 190–194 (1995).

36. Y. Saito *et al*., Differential NOVA2-mediated splicing in excitatory and inhibitory neurons regulates cortical development and cerebellar function. *Neuron* **101**, 707–720.e5 (2019).

37. W. Danysz, C. G. Parsons, Glycine and N-methyl-D-aspartate receptors: Physiological significance and possible therapeutic applications. *Pharmacol. Rev.* **50**, 597–664 (1998).

38. F. F. Johansen, J. Zimmer, N. H. Diemer, Early loss of somatostatin neurons in dentate hilus after cerebral ischemia in the rat precedes CA-1 pyramidal cell loss. *Acta Neuropathol.* **73**, 110–114 (1987).

39. N. Povysheva, A. Nigam, A. K. Brisbin, J. W. Johnson, G. Barrionuevo, Oxygen-glucose deprivation differentially affects neocortical pyramidal neurons and parvalbumin-positive interneurons. *Neuroscience* **412**, 72–82 (2019).

40. R. Hattori, K. V. Kuchibhotla, R. C. Froemke, T. Komiyama, Functions and dysfunctions of neocortical inhibitory neuron subtypes. *Nat. Neurosci.* **20**, 1199–1208 (2017).

41. N. H. Piguel *et al*., Scribble1/AP2 complex coordinates NMDA receptor endocytic recycling. *Cell Rep.* **9**, 712–727 (2014).

NEUROSCIENCE

Li et al.
Alternative splicing of GluN1 gates glycine site–dependent nonionotropic signaling by NMDAR receptors

PNAS | 11 of 11
https://doi.org/10.1073/pnas.2026411118